Preparation and characterization of nontoxic magnetic-luminescent nanoprobe*

Yin Nai-Qiang(尹乃强)[a], Liu Ling(刘 玲)[a], Lei Jie-Mei(雷洁梅)[a], Liu Yan-Song(刘艳松)[a], Gong Mao-Gang(公茂刚)[a], Wu Yi-Zhi(吴以治)[a], Zhu Li-Xin(朱立新)[b]†, and Xu Xiao-Liang(许小亮)[a]‡

[a] *Department of Physics, University of Science and Technology of China, Hefei* 230026, *China*
[b] *Center Laboratory, First Affiliated Hospital, Anhui Medical University, Hefei* 230022, *China*

(Received 4 May 2012; revised manuscript received 8 June 2012)

A novel nontoxic, magnetic, and luminescent nanoprobe is prepared by using complex nanoparticles, which are composed of Fe_3O_4 nanoparticles and Mn-doped ZnS quantum dots (QDs). The nanocomposite probe can provide visible optical and magnetic resonance images simultaneously. Compared with the previously toxic cadmium and mercury based QDs, the superiority of the Mn-doped ZnS QDs is little virulence. The structure and the properties of the particles are characterized by energy dispersive X-ray analysis spectroscopy, X-ray photoelectron spectroscopy, transmission electron microscopy, photoluminescence spectroscopy, and vibrating sample magnetometer.

Keywords: optical property, magnetic property, nanostructure

PACS: 61.05.C–, 78.55.–m, 75.75.–c, 68.37.Lp **DOI:** 10.1088/1674-1056/21/11/116101

1. Introduction

Semiconductor nanocrystals named quantum dots (QDs) have gained a lot of attention in the past few decades because of their outstanding optical properties and biological applications.[1,2] The spectral property of the QDs can be readily tuned by controlling the particle size as a result of the quantum-confinement effect. The main drawback of the traditional QDs is the toxicity and the low water solubility, which hinder their applications in biological systems. Various methods have been used to resolve the disadvantages. Core-shell QDs, such as CdSe/CdS/ZnS QDs,[3] can reduce the toxicity in a certain extent. Surface ligands of the hydrophobic QDs can be replaced by the amphiphilic ones[4,5] to increase their water soluilitiy. But these ligands will bring down the intensity of the photoluminescence. The synthesis of magnetic nanoparticles has also gained increasing attention due to their potential applications in drug delivery, magnetic separation,[6] and hyperthermia.[7−10] Nevertheless, the reactivity of iron oxide nanoparticles greatly increases as their dimensions are reduced, and the particles with relatively small sizes may undergo rapid biodegradation when they are directly exposed to biological environments. It has been demonstrated that suitable inert materials, such as silica, coated on the surfaces of iron oxide nanoparticles could prevent their aggregation in liquid and improve their chemical stability in biomedical applications.[11] Another advantage of the silica coating is that the surface is often terminated by silanol groups, which can covalently attach specific ligands to the surface and modify the surface chemistry of the particle.

Recently, increasing attention has been diverted to the fabrication of bifunctional nanostructures consisting of two kinds of materials with different properties, such as the nanoparticles possessing magnetic and luminescent properties.[12,13] In this paper, we introduce a way to synthesize a kind of nanocomposite composed of magnetic nanoparticles and nontoxic water-soluble fluorescent QDs. A new class of potential fluorescence biomedical label is introduced, which is based on transition metal manganese ion-doped quantum dots (d-dots) without heavy metal ions with ZnS as the host. The water-soluble nontoxic Mn-doped $ZnS/SiO_2/Fe_3O_4$ superparamagnetic luminescent nanocomposite (SPLNC) particles have a significant prospect in medical treatment because of their magnetic and luminescent bifunctional labels.

*Project supported by the National Natural Science Foundation of China (Grant Nos. 51272246 and 81172082).
†Corresponding author. E-mail: lx-zhu@163.com
‡Corresponding author. E-mail: xlxu@ustc.edu.cn
© 2012 Chinese Physical Society and IOP Publishing Ltd

2. Experiment

2.1. Materials

The materials used included absolute ethanol (99.7%), ammonia (25–28% NH_3, AR), hydrochloric acid (36% HCl), acetone (99.5%, AR), deionized water (18.25 $M\Omega \cdot cm^{-1}$), $FeSO_4 \cdot 7H_2O$ (99%), ferric chloride (97%), zinc acetate, sodium sulfide nonahydrate, manganese acetate, 3-mercaptopropionic acid, 3-aminopropyltrimethoxysilane (APS, Sigima), tetraethyl orthosilicate (TEOS) (28.4% SiO_2, AR), tetramethylammonium hydroxide solution (10% in water, Aldrich), and 3-mercaptopropionic acid (MPA, Sigima), where AR stands for the analytical reagent.

2.2. Preparation of Mn-doped ZnS quantum dots

In a typical experiment,[14] 5 mL of 0.1 M $Zn(NO_3)_2$, 1.5 mL of 0.01 M manganese acetate, and 20 mL of 0.1 M MPA were mixed together, then the solution was diluted to 45.5 mL with deionized water. The pH of the mixed solution was adjusted to 10.3 with 2 M NaOH. After the purging of air by N_2 bubbling for 30 min, 4.5 mL of 0.1 M Na_2S was quickly injected into the solution using a syringe. The mixture was kept for 15 min, and then the Mn-doped ZnS nanocrystals with 3 at.% Mn were aged at 50 °C for 2 h. After a hydrocooling process, the particles were purified with absolute ethanol and redispersed in 20 mL deionized water.

2.3. Preparation of colloidal Fe_3O_4 nanoparticles

The chemical coprecipitation method was used to prepare colloidal Fe_3O_4 nanoparticles. In brief, 2 mL of 4 M HCl was added to 10 mL of aqueous 1 M $FeCl_3$ (97%, Aldrich) and 5 mL of 1 M $FeSO_4$ under rapid mechanical stirring. Then 120 ml of 0.7 M NH_4OH (28–30%, Aldrich) was put into the mixed solution. After stirring for 30 min, the black solid product was allowed to precipitate. Then the product was dispersed in 20 mL distilled water, and subsequently 15 mL tetramethylammonium hydroxide solution (1 M) was added. Finally, the deionized water was added to the dispersion to obtain a solution of 150 mL.

2.4. Preparation of SiO_2/Fe_3O_4 nanoparticles

The modified Stöber method was introduced to prepare amorphous SiO_2 shell on the surface of the Fe_3O_4 nanoparticle. Firstly, magnetite nanoparticles were washed as follows. A 16 ml of magnetic-nanoparticles solution was added to 120 mL of deionized water containing 2 mL of HCl (0.01 M), the solution was centrifuged, and then the product was redispersed in pure water. Secondly, a part of the magnetic-nanoparticles solution was input to the mixture containing 6 mL of ammonia, 30 mL of deionized water, and 30 mL of absolute ethanol. Then an ethanolic solution of TEOS (0.75 mL of TEOS in 25 mL of absolute ethanol) was slowly added to the magnetic-nanoparticles solution. After stirring for 4 h at 40 °C, the magnetite-nanoparticles were centrifuged and then dissolved in 50 mL of deionized water.

2.5. Preparation of Mn-doped $ZnS/SiO_2/Fe_3O_4$

The linkage between SiO_2/Fe_3O_4 particles and Mn-doped ZnS QDs was based on the electrostatic interactions. At first, the magnetic nanoparticles were modified with APS, an ethanolic solution of APS (0.5 mL APS in 100 mL of absolute ethanol) was put into the SiO_2/Fe_3O_4 solution. The reaction was completed in 12 h at 60 °C, and the production was dissolved in 10 ml of deionized water. Then 2 mL of Mn-doped ZnS solution was slowly added into the modified SiO_2/Fe_3O_4 solution using a transfer pipette. The mixture was stirred for 6 h under rapid mechanical stirring. Finally, the solution was centrifuged, and the product was dissolved in 10 ml of deionized water.

2.6. Characterization

X-ray diffraction measurements were conducted with Cu $K\alpha$ (0.154 nm) serving as the incident radiation. The element analysis was conducted with the X-ray photoelectron spectroscopy (XPS). Microstructure and dimension of the nanoparticles were determined by a JEM-1400 transmission electron microscope with an acceleration voltage of 120 kV. The magnetic hysteresis loop was measured using a vibrating sample magnetometer (VSM; Quantum Design) at room temperature. Photoluminescence (PL) spectra were obtained by using an RF-5301 fluorescence spectrophotometer.

3. Results and discussion

Magnetic and luminescent Mn-doped ZnS/SiO_2/Fe_3O_4 nanocomposite particles were prepared basing on the Stöber method and the layer-by-layer (LbL) assembly, as outlined in Fig. 1.

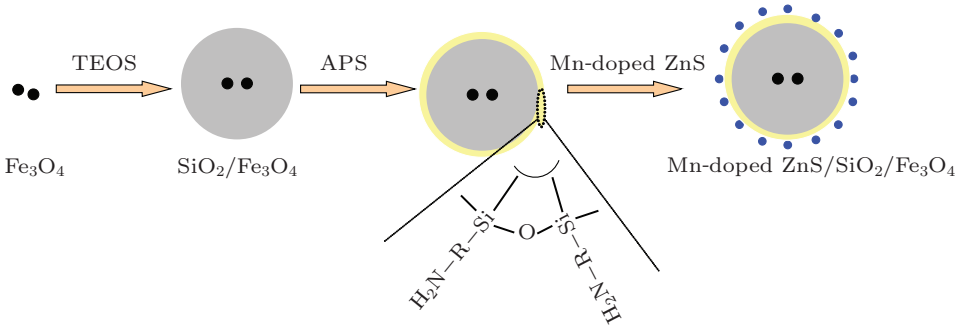


Fig. 1. (colour online) Schematic diagram of the preparation of the nanocomposite particles.

Figure 2 shows the XRD patterns of the bare Fe_3O_4, SiO_2/Fe_3O_4, Mn-doped ZnS, and Mn-doped ZnS/SiO_2/Fe_3O_4 nanoparticles. Five diffraction peaks can be indexed as (220), (311), (400), (511), and (440) planes of the cubic structure of Fe_3O_4, which match well with those in the standard card (JCPDS NO. 89-5892). In curve (ii) of Fig. 2, the strong broad peak around $2\theta = 25°$ results from the amorphous phase of silica. At the same time, the appearance of the five diffraction peaks of Fe_3O_4 indicates that SiO_2 has successfully assembled onto the Fe_3O_4 nanoparticles. In curve (iii) of Fig. 2, it is easy to distinguish the (111), (220), and (311) planes of cubic (zinc blende phase), which match well with those in the standard card of ZnS (JCPDS NO. 05-0566). From this diffractogram, the particle size of the Mn-doped ZnS is estimated to be 3.9 nm through the Scherrer equation. The pattern of the final Mn-doped ZnS/SiO_2/Fe_3O_4 nanoparticles shown in curve (iv) matches well with the combined pattern of Fe_3O_4, SiO_2, and Mn-doped ZnS. In the XRD pattern of the Mn-doped ZnS/SiO_2/Fe_3O_4 nanoparticles, the peak of the Mn-doped ZnS quantum dots is not obvious. To further explore the components of the nanocomparticles, XPS measurements were carried, the results are shown in Fig. 3. The Zn 2p, S 2p, and Mn 2p peaks are observed. Moreover, by XPS quantitative analysis, the concentrations of Zn 2p and S 2p in the Mn-doped ZnS/SiO_2/Fe_3O_4 nanoparticles are 3.09 at.% and 1.26 at.%, respectively. It indicates that the Mn-doped ZnS QDs are linked to the SiO_2/Fe_3O_4 nanoparticles successfully.

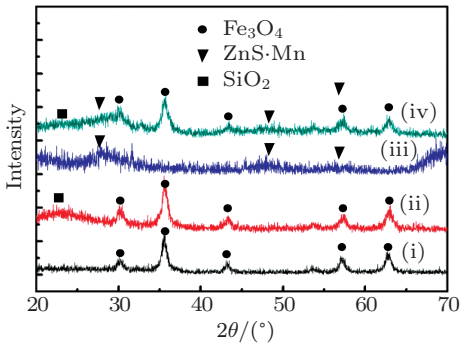


Fig. 2. (colour online) The power X-ray diffraction patterns of (i) bare Fe_3O_4, (ii) SiO_2/Fe_3O_4, (iii) Mn-doped ZnS, and (iv) Mn-doped ZnS/SiO_2/Fe_3O_4 nanoparticles.

In order to obtain detailed information about the microstructures and the morphologies of the bare Fe_3O_4, SiO_2/Fe_3O_4, and Mn-doped ZnS/SiO_2/Fe_3O_4 nanoparticles, the TEM observation was carried out, and the results are shown in Fig. 4. Due to the anisotropic dipolar attraction, the Fe_3O_4 MNPs tend to aggregate into large clusters, and thus lose their special magnetic properties. The tetra-methyl ammonium hydroxide (TMAH) is employed as a surfactant to reduce particle aggregation. The size of the prepared Fe_3O_4 is 12±3 nm with high uniformity (Fig. 4(a)). It shows that most of the bare Fe_3O_4 nanoparticles are quasi-spherical. Due to the large specific surface areas and the high surface energies, some nanoparticles still aggregate together. The diameter of SiO_2/Fe_3O_4 is in the range of 100–130 nm, and the surfaces of the nanoparticles look smooth (Fig. 4(b)). The SiO_2/Fe_3O_4 nanoparticles were prepared by a successive combination of the base-catalyzed hydrolysis and the condensation of

tetraethyl orthosilicate (TEOS) onto the iron oxide nanoparticles. The MNPs do not exist as individual particles, and some primary particles aggregate due to the magnetism of the nanoparticles. The thickness of the silica shell can be adjusted from a few to several hundred nanometers simply by varying the initial amount of TEOS. The diameter of the SiO_2/Fe_3O_4 nanoparticles employed here is in the range of 100–130 nm, and the surfaces of the nanoparticles are smooth (Fig. 4(b)). The TEM images (Fig. 4(c)) reveal the rougher surfaces of the silica-coated iron oxide nanoparticle as a result of Mn-doped ZnS quantum dots successfully self-assembled onto the surfaces of SiO_2/Fe_3O_4. The Mn-doped ZnS quantum dots are uniformly distributed on the SiO_2/Fe_3O_4 nanoparticles.

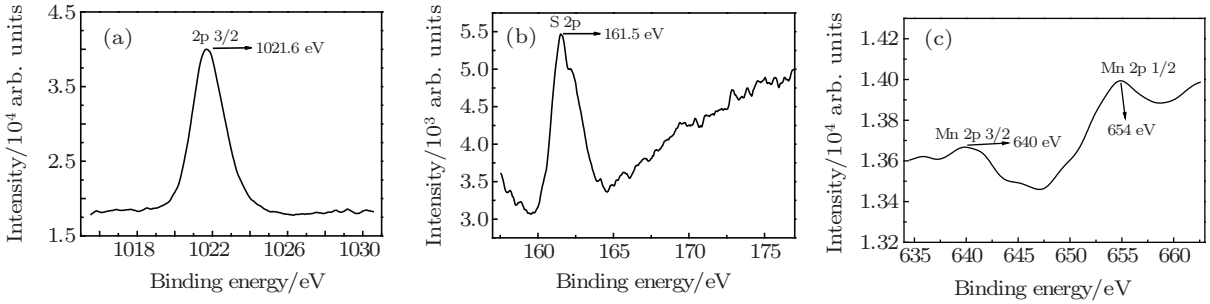


Fig. 3. XPS spectra of (a) Zn 2p, (b) S 2p, and (c) Mn 2p core levels of the Mn-doped $ZnS/SiO_2/Fe_3O_4$ nanoparticles.

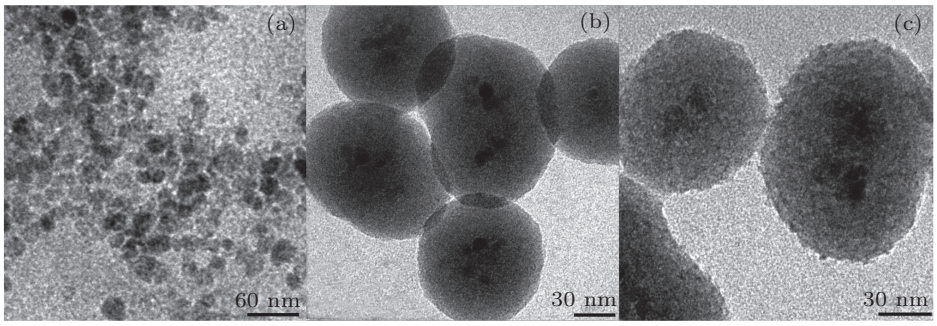


Fig. 4. TEM images of (a) bare Fe_3O_4, (b) SiO_2/Fe_3O_4, and (c) Mn-doped $ZnS/SiO_2/Fe_3O_4$ nano-particles.

Figure 5 shows the fluorescence spectra of the Mn-doped ZnS QDs before and after being coated on the SiO_2/Fe_3O_4 nanoparticles respectively. It is found that all spectra have two peaks, which correspond to the defect-state emission (around 460 nm) in the ZnS nanocrystals and the Mn^{2+} $^4T_1 \rightarrow {}^6A_1$ emission (around 570 nm). As reported in the the previous articles,[14,15] the peak intensity of the Mn^{2+} $^4T_1 \rightarrow {}^6A_1$ emission is higher than that of the defect-state emission when high-quality QDs are obtained.

The two emission spectra are blue-shifted (around 10 nm for both emission peaks) after assembling the Mn-doped ZnS QDs onto the surfaces of the magnetic silica spheres compared with those of the free QDs in the aqueous solution. This phenomenon is different from the previous observation that a red shift usually occurred when the other molecules were attached onto QDs and thus the sizes of the QDs increased. Cao *et al.*[16] and Wang *et al.*[17] also observed this phenomenon in the fabrication process of the nanocomposites. They reported the blue shifts[18,19] in luminescence spectra caused by the photoactivation processes that the QDs may have undergone, leading to the annealing/restructuring of their surfaces and thereby the removal of defects, since the photoactivation was accompanied by the photocorrosion. In our experience, there are two reasons leading to the phenomenon. On one hand, the thiol-capped Mn-doped ZnS QDs in solution shows higher photostability in the presence of an excess of the free thiol stabilizer. The thiol ligands of the Mn-doped ZnS QDs may be converted to disulfides under irradiation and during the layer-by-layer

process, producing unprotected Mn-doped ZnS QDs on the surfaces of the magnetic silica spheres, which would result in the size decrease of the Mn-doped ZnS QDs and the spectral shifts toward the shorter wavelengths. On the other hand, after the Mn-doped ZnS QDs are bound covalently to the surfaces of Fe_3O_4, the inter-particle spacing of the Mn-doped ZnS QDs is increased. Then the aggregation of the Mn-doped ZnS QDs is decreased, which in a way reduces the sizes of the Mn-doped ZnS QDs, resulting in the blue shifts in the fluorescence spectra.

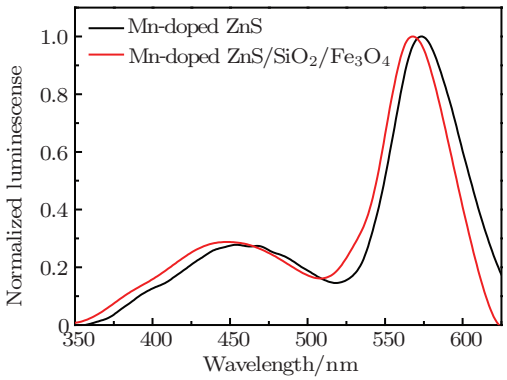


Fig. 5. (colour online) The PL spectra of bare Mn-doped ZnS and Mn-doped $ZnS/SiO_2/Fe_3O_4$ nanoparticles.

Rapid efficient collection has become one of the desired scientific goals with ramifications in immunoassay, bioseparation, and biolabeling applications. However, the conventional quantum-dot nanoparticles are difficult to realize. The SPLNC could resolve the problem due to the magnetic property of the magnetic luminescent nanocomposites. The magnetic properties of the silica-coated iron oxide spheres were recorded using a superconducting quantum interference device (SQUID) magnetometer with fields up to 8000 Oe, as shown in Fig. 6. The field-dependent magnetism at room temperature shows no coerciveforce and remanent magnetism, which exhibits the superparamagnetic characteristics desirable for their applications to delivery and separation.[20–23] The magnetization value can only reach a saturation moment of 7.0 emu/g, which is far less than the saturation magnetization of the magnetite/maghemite nanoparticles used for the preparation of these core/shell spheres (54 emu/g). It can be explained by the diamagnetic contribution of the thick silica shells surrounding the magnetic cores (the magnetic cores amount to only 2 wt.% of a magnetic silica sphere). The Mn-doped $ZnS/SiO_2/Fe_3O_4$ magnetic/fluorescent nanocomposites show slightly lower magnetization compared with the SiO_2/Fe_3O_4 magnetic nanocomposites due to the Mn-doped ZnS QDs surrounding the Fe_3O_4 magnetic core nanoparticles, which is consistent with the result reported in similar materials to CdSe quantum dots.[24,25] Figure 6 shows the photograph of an aqueous dispersion of luminescent magnetic spheres after an external magnetic field is introduced. The magnetic particles accumulate near the powerful magnet over a few minutes, while the particles are in uniform dispersion in the absence of the magnet. The magnetic particles are easily dragged to different positions by the powerful magnet. The magnetic properties allow the particles to efficient magnetic separation and magnetic site-specific transport under an external magnetic field in biomedical applications.

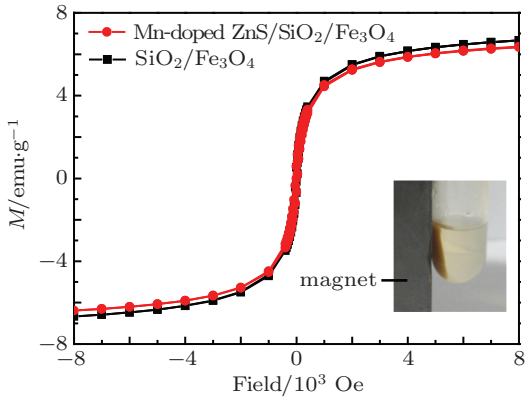


Fig. 6. (colour online) Magnetic curves of SiO_2/Fe_3O_4 and Mn-doped $ZnS/SiO_2/Fe_3O_4$ nanoparticles. The insert is the illustration of the magnet of the Mn-doped $ZnS/SiO_2/Fe_3O_4$ nanoparticles, which is absorbed near to the magnet aside.

4. Conclusion

In summary, we successfully synthesize the nontoxic, magnetic, and luminescent nanoprobe through Mn-doped ZnS QDs electrostatically assembled onto the amino-terminated SiO_2/Fe_3O_4 nanoparticles. These nanocomposites are expected to serve as luminescent markers when attached to bioligands and are capable of being driven by a magnetic field to a specific target.

References

[1] Weller H 1993 *Angew. Chem. Int. Ed.* **32** 41
[2] Alivisatos A P 1996 *J. Phys. Chem.* **100** 13226
[3] Deka S, Quarta A, Lupo M G, Claudio S, Giovanni M, Milena D G, Cinzia G, Roberto C and Liberato M 2009 *J. Am. Chem. Soc.* **131** 2948

[4] Pathak S, Choi S K, Arnheim N and Thompson M E 2001 *J. Am. Chem. Soc.* **123** 4103
[5] Chan W C W and Nie S 1998 *Science* **281** 2016
[6] Kim J, Lee J E, Lee J, Yu J H, Kim B C, An K, Hwang Y, Shin C H, Park J G, Kim J and Hyeon T 2006 *J. Am. Chem. Soc.* **128** 688
[7] Jordan A, Scholz R, Wust P, Fähling H and Felix R 1999 *J. Magn. Magn. Mater.* **201** 413
[8] Dennis C L, Jackson A J, Borchers J A, Ivkov R, Foreman A R and Hoopes P J 2008 *J. Phys.* D: *Appl. Phys.* **41** 13
[9] Mohammad F, Balaji G, Weber A, Uppu R M and Kuma C S S R 2010 *J. Phys. Chem.* C **114** 45
[10] Xu Z C, Hou L Y and Sun S H 2007 *J. Am. Chem. Soc.* **129** 8698
[11] Butterworth M D, Illum L and Davis S S 2001 *Colloids Surf.* A **179** 93
[12] Liu B, Wang D P, Huang W H, Yu M J and Yao A H 2008 *Materials Research Bulletin* **43** 2904
[13] Zhang R C, Liu L and Xu X L 2011 *Chin. Phys.* B **20** 8
[14] Zhuang J Q, Zhang X D, Wang G, Li D M, Yang W S and Li T J 2003 *J. Mater. Chem.* **13** 1853
[15] Xiao Q and Xiao C 2008 *Appl. Surf. Sci.* **254** 6432
[16] Cao X B, Lan X M, Guo Y, Zhao C, Han S M and Wang J 2007 *J. Phys. Chem.* C **111** 18958
[17] Wang D S, He J B, Rosenzweig N and Rosenzweig Z 2004 *Nano Lett.* **3** 409
[18] Liu B, Xie W X, Wang D P, Huang W H, Yu M J and Yao A H 2008 *Materials Letters* **62** 3014
[19] Yan H and Zhang J C 2010 *Acta Materialia* **58** 726
[20] Bean C P and Livingston J D 1959 *J. Appl. Phys. Suppl.* **30** 120
[21] Long Y Z, Chen Z J, Liu Z X, Zhang Z M, Wan M X and Wang N L 2003 *Chin. Phys.* **12** 433
[22] Sathe T R, Agrawal R and Nie S M 2006 *Anal. Chem.* **78** 5627
[23] Hong X, Li J, Wang M J, Guo W, Li J H, Bai Y B and Li T J 2004 *Ter.* **16** 4027
[24] Yi D K, Selvan S, Lee S S, Papaefthymiou G C, Kundaliya D and Ying J Y 2005 *J. Am. Chem. Soc.* **127** 4990
[25] Feng W C, Gao R W, Li W, Han G B and Sun Y 2005 *Chin. Phys.* **14** 1649